CHEMISTRY
A EUROPEAN JOURNAL

DOI: 10.1002/chem.200902973

Single-Crystalline ZnO Nanowire Bundles: Synthesis, Mechanism and Their Application in Dielectric Composites

Guangsheng Wang,*[a, b] Yuan Deng,*[a] and Lin Guo*[a]

Abstract: Single-crystalline ZnO nanowire bundles have been synthesized in large-scale by an improved microemulsion method in the presence of excessive hydrate hydrazine and dodecyl benzene sulfonic acid sodium salt (DBS) in xylene. The product is characterized using X-ray diffraction (XRD), scanning electron microscopy (SEM), transmission electron microscopy (TEM), and high-resolution transmission electron microscopy (HRTEM). The result shows that the bundle is composed by many oriented single-crystalline ZnO nanowires with a length of about 1 μm and a diameter of about 20–30 nm. The influence of DBS, hydrazine and the reaction time on the morphology of final product and the formation mechanism of such nanostructures were discussed; the application in the dielectric composites is also studied.

Keywords: dielectric composites · microemulsion method · nanotechnology · nanowires · zinc

Introduction

As an important wide-band-gap semiconductor with $E_g = 3.37$ eV, ZnO has been of great research interest as a result of its unique applications in catalysts, sensors, piezoelectric transducers and actuators, and photovoltaic and surface acoustic wave devices.[1,2] For these applications, the morphology control of ZnO structures is critical in order to tune their chemical and physical properties to the appropriate ones. ZnO nanobelts,[3,4] nanorings and nanorows,[5,6] nanowires,[7–9] nanocombs,[10] have been reported and various synthetic methods have been developed to prepare ZnO nanomaterials, such as vapor–liquid–solid epitaxial (VLSE) mechanism,[11] thermal evaporation,[12] hydrothermal methods,[13] template-based growth,[14] chemical-vapor deposition,[15] pulsed-laser deposition[16] and micro-emulsion,[17] but it is still a challenge to synthesis arrays in solution at low temperature.

Recently, ZnO nanoparticles has been studied as a conductive-filler in polymer[18] for the polymer/matrix composites with high dielectric permittivity have received increasing interest recently for various potential applications in high charge-storage capacitor.[19] A wide variety of high dielectric constant composite materials have been developed. Efforts to improve the overall dielectric performance of these materials have been devoted to maximize the dielectric constant and suppress the dielectric loss. Two methods were employed currently for improving the dielectric constant of the polymers. One is to disperse some ferroelectric ceramic powders into the polymer to form 0–3 type composites. Adopt traditional ceramics, for example, $BaTiO_3$, $BaSrTiO_3$, $PbZrTiO_3$, CCTO, have been actively explored as fillers.[20–24] The effective dielectric constant of the ferroelectric ceramic–polymer composites increases with the volume fraction of the ceramics based on the mixing rules. While the dielectric constant of these polymer–ceramic composites developed to date is either below 100 or high but with high filler content at room temperature.

The other significant efforts have focused on developing percolative composites. Conductive filler/polymer composite is another approach towards high dielectric constant materials, which is a kind of conductor–insulator composite based on percolation theory. Ultra-high dielectric constant can be

[a] Dr. G. Wang, Prof. Dr. Y. Deng, Prof. Dr. L. Guo
School of Chemistry & Environment, BeiHang University
Beijing 100191 (P.R. China)
E-mail: wanggsh@ustc.edu.cn
dengyuan@buaa.edu.cn
guolin@buaa.edu.cn

[b] Dr. G. Wang
Division of Nanomaterials & Chemistry
Hefei National Laboratory for Physical Sciences at Microscale Structural Research Laboratory of CAS
University of Science and Technology of China
Hefei 230026 (P.R. China)

expected with conductive filler/polymer composites when the concentration of the conductive filler is approaching the percolation threshold. And also this percolative approach requires much lower volume concentration of the filler compared to traditional approach of high dielectric constant particles in a polymer matrix. Therefore, this material option represents advantageous characteristics over the conventional ceramic/polymer composites. Various conductive fillers, such as silver (Ag), aluminum (Al), nickel (Ni), carbon black, have been used to prepare the polymer–conductive filler composites.[25–32] The ZnO/polymer composites were always thought as a material with low dielectric constants, but no percolation threshold was found by adding ZnO nanoparticles (49 nm) into low density polyethylene (LDPE) ever at high filler content; While, the dielectric property of composites depends on physical property, preparation method, and interface interaction between the fillers and the polymer, especially the morphologies of fillers. New insights into the unique properties of the nanoparticle filler and polymer matrix have been gained in most recent studies.[33] An increase of the dielectric properties is still a challenge.

In this paper, we synthesized ZnO nanoparticles with a shape of ZnO nanowire bundles by an improved microemulsion at low temperature, and investigate the mechanism and their application in dielectric composites.

Results and Discussion

Characterization and controllable synthesis of ZnO nanowire bundles: ZnO nanowire bundles were synthesized by the reflux for 5 h with R_D ($R_D=8$) and R_H ($R_H=40$). Powder XRD pattern of as-prepared products is shown in Figure 1a. All diffraction peaks can be indexed as those from the known Wurtzite-structured (hexagonal) ZnO (JCPDS 75-1526). Figure 1b shows the product reflux time is reduced to 1 h at the same conditions, no ZnO but $Zn(OH)_2$ and $Zn(CH_3COO)_2$ were detected, which mean $Zn(OH)_2$ would be formed as an intermediate during the microemulsion approach.

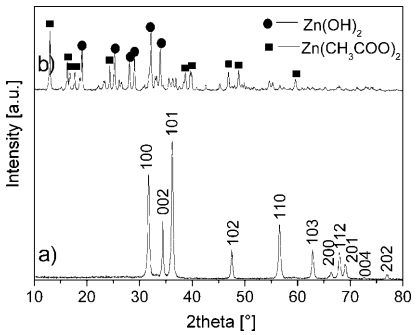

Figure 1. XRD patterns of the product heated under reflux for a) 5 h and b) 1 h.

A general overview of the product (shown in Figure 2a) indicates the material consists of uniformed bundles with a length of about 1 μm. The nanowires composed of the bundle grow uniformly along the same direction. A closer examination of the bundle (shown in Figure 2b) indicates that the bundle consists of large quantities of uniform wires with a length of about 1 μm and a diameter of about 20–30 nm. In order to confirm the elements of the sample, a typical energy dispersive spectroscopy (EDS) recorded on one nanowire was given as insert of Figure 2a. No other elements can be detected from spectrum except for Zn and O (Au and C came from the electric colloid used to support the sample).

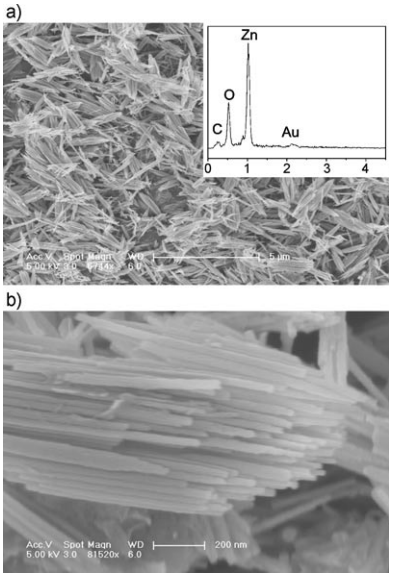

Figure 2. SEM image of the product: a) a general overview, the inset is a typical EDS composition analysis of a selected area (scale bar = 5 μm); b) enlarged ZnO nanowire bundle (scale bar = 20 nm).

Additional structural characterization of the ZnO nanowire bundles is carried out using TEM and HRTEM. The TEM image (Figure 3a) shows the typical image of the individual ZnO bundle nanostructures are stable even after a long time of ultrasonic, indicating that there maybe some chemical bonding among the nanowires. HRTEM images (Figure 3b), taken from the selected area marked by a square in Figure 3a, reveal that the nanowires possess a single crystal structure. The inset of Figure 3b is the corresponding processed (fast Fourier transform) FFT of the image Figure 3b also indicates that the nanowires are single crystal. The enlarged HRTEM image (shown in Figure 3c) shows that the entire lattice in two contiguous nanowires have almost the same spacing and direction where the singular spacing is 0.26 nm, which is nearly consistent with the (002) reflection plane spacing of the hexagonal ZnO phase. The $<001>$ direction marked by the white arrows was parallel to the long axis of the rods, indicating that the $<001>$ direction is a common growth direction for the ZnO nano-

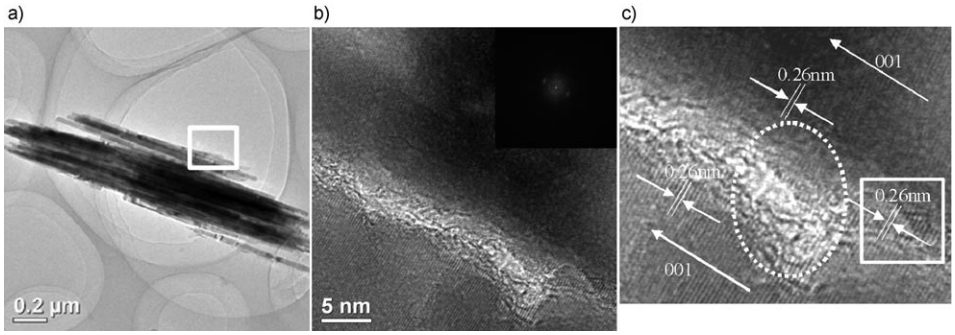

Figure 3. a) TEM image of the ZnO nanowire bundles; b) HRTEM image of the selected area marked by a square in a), insert is FFT of the image b); c) enlarged HRTEM image of the selected area marked by a square in b).

wires. The side view of nanowires is also shown in Figure 3c, the difference in brightness, marked by a round, indicates that the joints of wires are thin. The nanowires are directly connected by crystalloid, marked by a square, and aligned not only in length direction but also in crystallography orientation.

The optimized reaction condition to prepare ZnO nanowire bundles is the reflux of $Zn(CH_3COO)_2{\cdot}2H_2O$, dodecyl benzene sulfonic acid sodium salt (DBS) and hydrate hydrazine for 5 h in a solution of xylene with $R_H = 40$ and $R_D = 8$.

In this reaction, R_D is an important factor to affect the final structure. When the molar ratio of DBS to $Zn(CH_3COO)_2{\cdot}2H_2O$), R_D was reduced to 0.85 and the resulting ZnO exhibits bundles composed of several nanorods and some dispersed thickset rods (shown in Figure 4a). When R_D was decreased to 5.7, the bundles composed of nanowires with the diameter about 30–50 nm and length about 1.5–2.5 μm can be obtained (shown in Figure 4b). Compared with typical products shown in Figure 2, the diameter of the ZnO nanowires thus decreases and the conglomeration increases with the increasing R_D.

$\mathbf{R_H}$ would affect the diameter of the nanostructures during the following growth process, which also determine the size of the droplet. When the reaction was performed under the same reaction conditions but only increasing R_H to 50, the product was composed of bundles; some exhibit radial structures (Figure 4c), which may be due to the superabundant hydration agent hydrazine, which led to increased nucleation and growth to form radial nanowires with Zn^{2+}. When the reaction was performed under the same condition but a decreased R_H value of 20, the product was mainly composed of dispersed ZnO nanowires; some bundles consisted of nanowires with a diameter of about 100 nm (Figure 4d). The diameter of nanowires and the morphologies of ZnO particles can easily be adjusted by changing the R_H value. These results also indicate that the aggregation of the bundles decrease with the decreasing of R_H.

The influence of reflux time was also studied. The products do not contain ZnO but column-like $Zn(OH)_2$ (XRD shown in Figure 1b) with the chapped ends (Figure 4e) when reflux time was above 1 h; this implies that $Zn(OH)_2$ would be the intermediate during the microemulsion approach. Most of the bundles structures were dispersed, and the diameter of the nanowires enhanced (Figure 4f) when reflux time was above 8 h.

From experiments above mentioned, we can conclude that the R_D, R_H and reaction time play an important role on the growth of ZnO particles with varies morphologies. In this process, R_D and R_H are the key factor to the final bundles structure.

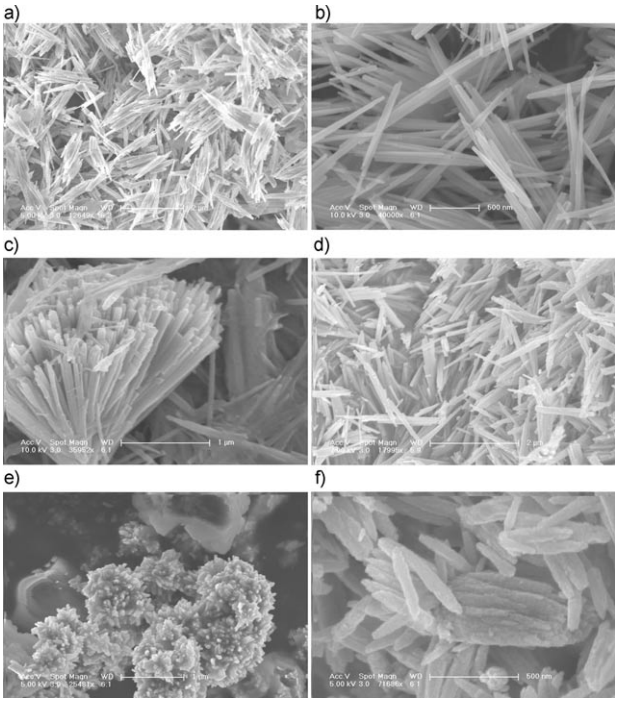

Figure 4. a) Product prepared with an R_D value decreased to 0.85 (scale bar = 2 μm); b) the product prepared with R_D decreased to 5.7 (scale bar = 500 nm); c) product prepared with R_H increased to 50 (scale bar = 1 μm); d) product prepared with R_H decreased to 20 (scale bar = 2 μm); e) product reflux for 1 h (scale bar = 1 μm); f) product reflux for 8 h (scale bar = 500 nm).

Reaction and growth mechanism: The overall reaction in the current system could be simply formulated as follows:

$$Zn^{2+} + 2N_2H_4 \cdot H_2O \rightleftharpoons Zn(OH)_2\downarrow + 2N_2H_5^{+} \quad (1)$$

$$Zn(OH)_2 \rightleftharpoons ZnO + H_2O \quad (2)$$

From the observation of the experiments mentioned above, we can conclude that the possible mechanism of the bundle

structure can be described with the following stages (Figure 5). At the first stage (Figure 5a), the reactants-containing solution enwrapped by the capping molecules acts as a wirelike-microreactor (Figure 5a), then the excess $N_2H_5^+$ ions are adsorbed on the surface of the resulting wirelike-microreactors, and then $Zn(OH)_2$ column blocks are formed (Figure 4f). During the 5 h reflux, $Zn(OH)_2$ decomposes in the wirelike-microreactors and the ZnO nanowires are formed (Figure 5b). The microreactors formed column blocks before being ruptured after the reflux process; the ZnO nanowires are located between the linked wirelike-microreactors and connected with each other by crystalloid structures, which leads to bundle formation (Figure 5c), which has been proved in the HRTEM measurements.

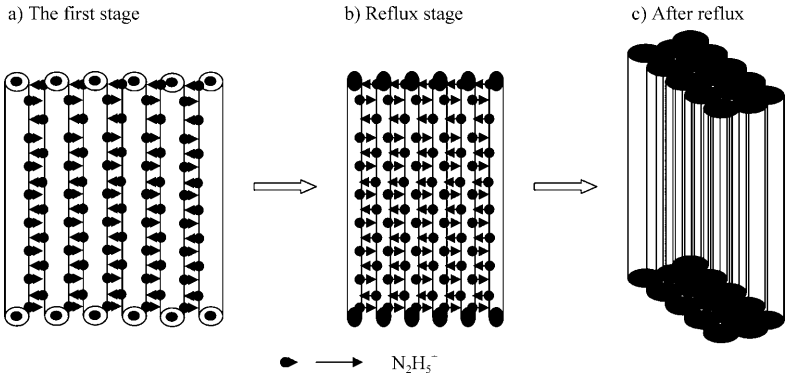

Figure 5. Growth mechanism of the ZnO nanowire bundles

Dielectric properties: To investigate how the bundles nanostructures affect the dielectric properties of composites, various contents of ZnO bundles powder were mixed with poly(vinylidene fluoride) (PVDF) to form ZnO/PVDF composites by hot-press process. Excellent dispersion of ZnO bundles; the compact structure in the polymer is shown in the SEM images of the composites in Figure 6. The interface between ZnO bundles and polymer was eliminated, which may due to the use of DBS in the synthesis process. The ZnO bundles were still kept radial shape in the composites after the hot-press.

For comparison, the dielectric properties of various contents of bulk ZnO/PVDF (ZnO/PVDF) composites were measured at room temperature, which is shown in Figure 7.

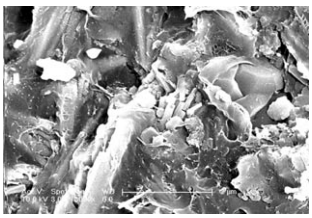

Figure 6. A cross-sectional SEM image of the wafers of the composite with the filler content 15 wt% (scale bar = 2 μm).

The used bulk ZnO is composed of nanoparticles with a length of about 200–300 nm. The dielectric constants of the composites decrease with the increase frequency (Figure 7a). The relationship of the dielectric constants and filler content of ZnO, which indicates the dielectric constant slowly increase with the increasing weight ratio; there exists no percolation threshold by adding ZnO nanoparticles into PVDF in the considerable range, which is the same result as the reported ZnO/LDPE.[18] The dielectric loss is no higher than 0.2 from 10^3 to 10^6 Hz.

Compared with ZnO/PVDF, the dielectric constants of the ZnO bundles/PVDF improved considerably (Figure 8a), which may be based on the bundle nanostructures. The dipole–

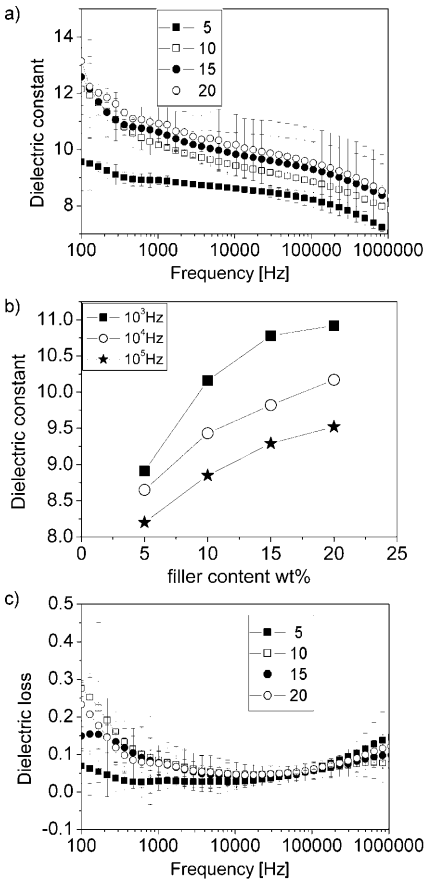

Figure 7. Dielectric constant and dielectric loss measured at different frequencies for the composites (bulk-ZnO/PVDF) mixed with different wt% at the room temperature: a) The dielectric constant. b) Variation of dielectric constant of the different filler content (wt%) of ZnO at the frequency of 10^3, 10^4, 10^5 Hz. The data presented of c) is the same as a). c) Dielectric loss.

dipole interaction increased and contributed to higher dielectric constant. This implies that the incorporation of ZnO nanowires bundles into PVDF is also effective to increase its dielectric constant, which is the same result as the reported R-ZnO/PVDF.[33] A low percolation threshold is observed for ZnO bundles/PVDF nanocomposites (insert of Figure 8a), at a critical filler content 15wt%, where the dielectric constant abruptly increases. The dielectric constant of the percolation composites reaches 96 at 10^2 Hz, which are significantly eight times higher than that of bulk-ZnO/PVDF composites with the same filled content. There are two reasons for the increased dielectric constant: one is that the significant increase of the dielectric constant is ascribed to a whole conductive network formed eventually in the composites when the volume fraction of the ZnO bundles fillers increases to the threshold (15wt.%); the other is that the dielectric constant of a material is a function of its capacitance, which is also proportional to the quantity of charge stored on either surface of the sample under an applied electric field, the polarization of the ZnO/PVDF interfaces makes an additional contribution to the charge quantity. Therefore, the higher dielectric constant appears in the composites with a higher volume fraction of ZnO bundles.[34]

The variation of dielectric loss with frequency is also depicted in Figure 8b. It is noted that the dielectric loss of the percolation ZnO bundles/PVDF composite is as high as 0.5 at room temperature in the region of 10^2–10^3 Hz. Furthermore, towards higher frequency, the dielectric loss of the percolation composite is lower than 0.25 with an increase in frequency 10^5 Hz, for the percolation composites, the dielectric loss increases rapidly. Usually, the introduction of inorganic semiconductor fillers to a polymer matrix enhances the dielectric loss values of the composites.[35]

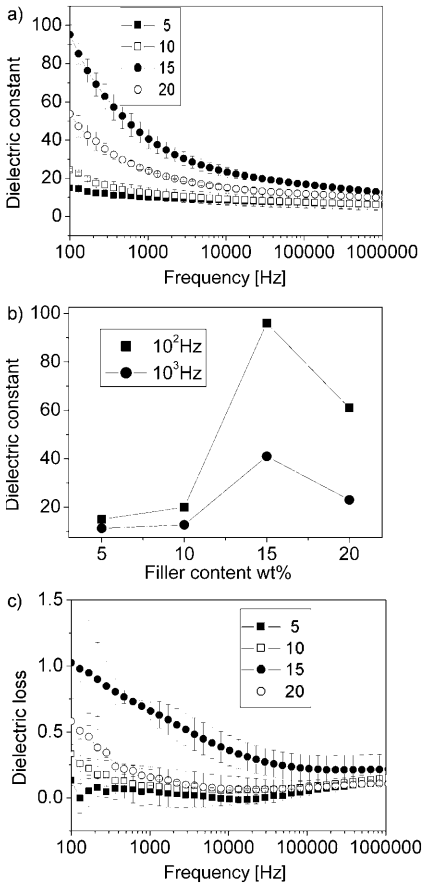

Figure 8. Dielectric constant and dielectric loss measured at different frequencies for the composites (ZnO bundles/PVDF) mixed with different wt% at the room temperature: a) The dielectric constant. b) Variation of dielectric constant of the different filler content (wt%) of ZnO bundles at the frequency of 10^2, 10^3 Hz. The data presented of c) is the same as a). c) Dielectric loss.

Conclusion

In summary, we have demonstrated a new approach to synthesize ZnO nanowire bundles. The nanowires composed of the bundles are aligned not only in length direction but also in crystallography orientation. This method shows the possibility of growing in large scale ZnO nanowires arrays by a microemulsion method at low temperature. The nanowire bundles should be of interest for applications of such structures in displays, in microlasers, and in photonics devices. The ZnO bundles/PVDF composites have significantly higher dielectric constants compared with those of bulk ZnO/PVDF, with a quite low percolation threshold. This also confirmed that one-dimensional ZnO nanostructures can enhance the dielectric constant of polymers. It is a promising dielectric composite with high dielectric constant and low inorganic filler content.

Experimental Section

Commercially available and analytical-grade reagents were used without further purification. $Zn(CH_3COO)_2{\cdot}2H_2O$ (1.1 g) was dissolved in xylene (150 mL), then the dodecyl benzene sulfonic acid sodium salt (DBS) with the different molar ratio R_D [R_D=(surfactant/$Zn(CH_3COO)_2{\cdot}2H_2O$)] from 0 to 8 were added successively. After the solution was vigorous stirred for 1 h at room temperature, 50% hydrazine with the different molar ratio R_H [R_H=(hydrazine/$Zn(CH_3COO)_2{\cdot}2H_2O$)] from 10 to 50 were added to the mixed transparent solution and refluxed for 5 h. Then, the white precipitates were collected, washed with ethanol and distilled water several times, and then dried in the oven at 70°C.

A series of PVDF (0.475, 0.450, 0.425, and 0.400 g) were dissolved in *N*-dimethylformamide (40 mL) at room temperature. After the solution turned transparent, the ZnO bundles or bulk ZnO (0.025, 0.050, 0.075, and 0.100 g), were added, respectively, then dispersed by ultrasonic bath treatment at room temperature. Then the sample was dried in the oven at 80°C. The dried mixture was compressed into wafers for 25 min at 200°C under 10 MPa (pre-pressed for 5 min at the same temperature. The press was released for a short period of time and then re-pressed for 20 min, followed by cooling to room temperature under the same pressure).

Powder XRD data were collected on a Rigaku D/MAX 2200 PC automatic X-ray diffractometer with $Cu_{K\alpha}$ radiation (λ=0.154056 nm). The grain morphology and size was observed by SEM (FEI Siron 200) and

TEM (HITACHIH-8100). Further structural and elemental analyses were performed using HRTEM (FEI Company, Tecnai G2 F20S-Twin FEG TEM at 300 kV) and selected area electron diffraction (SAED). The dielectric constants were measured by a HP 4294 A Impedance meter in the frequency range of 100/11 MHz, at an average voltage of 0.5 V under the room temperature.

Acknowledgements

The work was supported by National Natural Science Foundation of China under Grant No. 50772005, 50725208 and 20973019, Beijing Technology Topic Program under Grant No. Z08000303220808, the National High Technology Research and Development Program of China under Grant No. 2009AA03Z322, and the National Science Foundation for Postdoctoral Scientists.

[1] Z. Zhang, H. Yu, X. Shao, M. Han, *Chem. Eur. J.* **2005**, *11*, 3149–3154.
[2] P. Fei, P. H. Yeh, J. Zhou, S. Xu, Y. F. Gao, J. H. Song, Y. D. Gu, Y. Y. Huang, Z. L. Wang, *Nano Lett.* **2009**, *9*, 3435–3439.
[3] J. M. Zhang, C. Yu, Z. M. Liao, X. Z. Zhang, L. P. You, D. P. Yu, *J. Electron Microsc.* **2009**, 58, 295–299.
[4] Y. K. Park, A. Umar, E. W. Lee, D. M. Hong, Y. B. Hahn, *J. Nanosci. Nanotechnol.* **2009**, *9*, 5745–5751.
[5] X. Y. Kong, Y. Ding, R. Yang, Z. L. Wang, *Science* **2004**, *303*, 1348.
[6] W. L. Hughes, Z. L. Wang, *J. Am. Chem. Soc.* **2004**, *126*, 6703.
[7] X. D. Shan, X. Z. Zhang, J. Y. Gao, L. P. You, H. J. Xu, J. Xu, D. P. Yu, H. Q. Ye, *J. Phys. Chem. A* **2009**, *113*, 18014–18019.
[8] Z. L. Wang, *Mater. Sci. Eng. R* **2009**, *64*, 33–71.
[9] Y. Ding, Z. L. Wang, *Micron.* **2009**, *40*, 335–342.
[10] A. Umar, *Nanoscale Res. Lett.* **2009**, *4*, 1004–1008.
[11] C. Thiandoume, J. Barjon, O. Ka, A. Lusson, P. Galtier, V. Sallet, *J. Cryst. Growth.* **2009**, *311*, 4311–4316.
[12] R. Yousefi, B. Kamaluddin, *Appl. Surf. Sci.*. **2009**, *256*, 329–334.
[13] W. W. Lin, D. G. Chen, J. Y. Zhang, Z. Lin, J. K. Huang, W. Li, Y. H. Wang, F. Huang, *Cryst. Growth Des.* **2009**, *9*, 4378–4383.
[14] C. H. Lai, W. F. Lee, I. C. Wu, C. C. Kang, D. Y. Chen, L. J. Chen, P. T. Chou, *J. Mater. Chem.* **2009**, *19*, 7284–7289.
[15] D. Wang, J. W. Zhang, Y. N. Hu, G. M. Li, Z. Bi, X. A. Zhang, X. M. Bian, X. Hou, *Mater. Lett.* **2009**, *63*, 2157–2159.
[16] W. W. Li, Z. G. Hu, J. D. Wu, J. Sun, M. Zhu, Z. Q. Zhu, J. H. Chu, *J. Phys. Chem. A* **2009**, *113*, 18347–18352.
[17] Y. Deng, G. S. Wang, N. Li, L. Guo, *J. Lumin.* **2009**, *129*, 55–58.
[18] J. I. Hong, P. Winberg, L. S. Schadler, R. W. Siegel, *Mater. Lett.* **2005**, *59*, 473–476.
[19] J. X. Lu, C. P. Wong, *IEEE Trans. Dielectr. Electr. Insul.* **2008**, *15*, 1322–1328.
[20] H. L. W. Chan, M. C. Cheung, C. L. Choy, *Ferroelectrics* **1999**, *224*, 113–120.
[21] R. Gregorio, M. Cestari, F. E. Bernardino, *J. Mater. Sci.* **1996**, *31*, 2925–2930.
[22] Y. Rao, S. Ogitani, P. Kohl, C. P. Wong, *J. Appl. Polym. Sci.* **2002**, *83*, 1084–1089.
[23] Z. M. Dang, Y. H. Lin, C. W. Nan, *Adv. Mater.* **2003**, *15*, 1625–1629.
[24] M. Arbatti, X. B Shan, Z. Y. Cheng, *Adv. Mater.* **2007**, *19*, 1369.
[25] L. Wang, Z. M. Dang, *Appl. Phys. Lett.* **2005**, *87*, 042903.
[26] Z. M. Dang, L. Wang, Y. Yin, Q. Zhang, Q. Q. Lei, *Adv. Mater.* **2007**, *19*, 852–857.
[27] L. Qi, B. I. Lee, S. Chen, W. D. Samuels, *Adv. Mater.* **2005**, *17*, 1777–1781.
[28] J. Lu, K. S. Moon, J. Xu, C. P. Wong, *J. Mater. Chem.* **2006**, *16*, 1543–1548.
[29] J. X. Xu, C. P. Wong, *Appl. Phys. Lett.* **2005**, *87*, 082907.
[30] Z. M. Dang, Y. Shen, C. W. Nan, *Appl. Phys. Lett.* **2002**, *81*, 4814.
[31] H. W. Choi, Y. W. Heo, J. H. Lee, J. J. Kim, H. Y. Lee, E. T. Park, Y. K. Chung, *Appl. Phys. Lett.* **2006**, *89*, 132910.
[32] J. X. Xu, C. P. Wong, Proceedings of the 54th IEEE Electronic Components and Technology Conference, **2004**, p. 536.
[33] G. S. Wang, Y. Deng, Y. Xiang, L. Guo, *Adv. Funct. Mater.* **2008**, *18*, 2584–2591.
[34] Z. M. Dang, J. P. Wu, H. P. Xu, S. H. Yao, M. J. Jiang, *Appl. Phys. Lett.* **2007**, *91*, 072912.
[35] S. Singha, M. J. Thomas, *IEEE Trans. Dielectr. Electr. Insul.* **2008**, *15*, 12–23.

Received: October 27, 2009
Revised: March 24, 2010
Published online: June 29, 2010

